

Temperature dependence of electron transfer in coupled quantum wells

Amlan Majumdar^{a)}

Department of Electrical Engineering, Princeton University, Princeton, New Jersey 08544

K. K. Choi

U.S. Army Research Laboratory, Adelphi, Maryland 20783

J. L. Reno

Sandia National Laboratories, Albuquerque, New Mexico 87185

L. P. Rokhinson and D. C. Tsui

Department of Electrical Engineering, Princeton University, Princeton, New Jersey 08544

(Received 9 October 2002; accepted 4 December 2002)

We report on the temperature dependence of electron transfer between coupled quantum wells in a voltage tunable two-color quantum-well infrared photodetector (QWIP). The detection peak of this QWIP switches from $7.1\ \mu\text{m}$ under positive bias to $8.6\ \mu\text{m}$ under negative bias for temperatures $T \leq 40\ \text{K}$. For $T \geq 40\ \text{K}$, the $7.1\ \mu\text{m}$ peak is present under both bias polarities and increases significantly with T while the $8.6\ \mu\text{m}$ peak decreases correspondingly. We determine the temperature dependence of electron densities in the two QWs from the detector absorption spectra that are deduced using corrugated QWIPs and find that electron transfer is efficient only when thermionic emission is not significant. © 2003 American Institute of Physics.

[DOI: 10.1063/1.1541094]

Voltage tunable two-color quantum-well infrared photodetectors (QWIPs) have many important applications such as remote temperature sensing.^{1,2} These two-terminal detectors when integrated with time-multiplexed readout circuits greatly simplify focal plane array production. Most voltage tunable detectors demonstrated so far are based on electric field induced Stark shift and usually have small tuning ranges.³ Another tuning mechanism is electron transfer between coupled QWs under an applied bias.⁴ In these detectors, two unequal QWs are coupled through a thin barrier of thickness t_a (with single electron tunneling rate r_a) to form an unit cell. The entire structure consists of a number of unit cells separated by larger barriers of thickness t_b (with electron tunneling rate r_b). In earlier designs with $t_a \sim 50\ \text{Å} \ll t_b \sim 500\ \text{Å}$, the condition $r_a \gg r_b$ resulted in thermal equilibrium and a common Fermi level within each unit cell.^{5,6} Due to the small potential drop between the QW pair, the amount of electron transfer was insufficient to switch the peak detection wavelength. We showed that the potential drop and, hence, electron transfer between the QW pair is enhanced by increasing t_a relative to t_b .⁷ Subsequently, we demonstrated a two-color detector where the peak wavelength switched from 7.5 to $8.8\ \mu\text{m}$ upon reversing the bias polarity at low temperatures.⁸

The earlier-mentioned approach of enhancing electron transfer between QWs has certain limitations. Increasing t_a/t_b reduces r_a/r_b so that the QW pair is driven away from thermal equilibrium under bias, which tends to reduce electron transfer. When tunneling between the QWs is not sufficiently strong, electron transfer can be affected by temperature T if $t_a \neq t_b$. When T increases, the electron transfer rate, which includes all transport mechanisms, can change differ-

ently for the two QWs within each QW pair because of different thermal activation energies. Therefore, the electron population in each QW can have a rich functional dependence on both detector parameters and experimental conditions.

In this letter, we present the temperature dependence of electron transfer in a voltage tunable detector, where the peak wavelength $\lambda_p = 7.1\ \mu\text{m}$ under positive bias and switches to $\lambda_p = 8.6\ \mu\text{m}$ under large negative bias below $T = 40\ \text{K}$. At higher temperatures, the shorter wavelength peak becomes apparent even under negative bias and its magnitude grows with T , while the longer wavelength peak decreases correspondingly. We deduce the detector absorption spectra under different experimental conditions using corrugated QWIPs^{9,10} and use these spectra to determine the electron densities in the two QWs at different temperatures. We find that the electron transfer process is efficient only when thermionic emission is not significant.

The detector structure consists of 36 periods of QW pairs sandwiched between heavily doped top and bottom GaAs contact layers. Each period consists of a $44\ \text{Å}$ $\text{Al}_{0.05}\text{Ga}_{0.95}\text{As}$ left QW (LQW) coupled to a $44\ \text{Å}$ GaAs right QW (RQW) through a $200\ \text{Å}$ $\text{Al}_{0.3}\text{Ga}_{0.7}\text{As}$ barrier and separated from the next set of QW pair by a $350\ \text{Å}$ graded $\text{Al}_x\text{Ga}_{1-x}\text{As}$ barrier ($x = 0.3 \rightarrow 0.25$ along the growth direction). The LQWs are uniformly doped with $7 \times 10^{17}\ \text{cm}^{-3}$ Si donors while the RQWs and the barriers are undoped. The entire structure is grown on (100)-GaAs by molecular beam epitaxy. The conduction band diagram of an unit cell of the detector is sketched in Figs. 1(a)–1(b). In this structure, electrons are expected to be in the LQW at large negative bias and be transferred to the RQW under positive bias. We calculated the oscillator strength f of different intersubband transitions from the ground states of both QWs to the excited states

^{a)}Electronic mail: majumdar@ee.princeton.edu

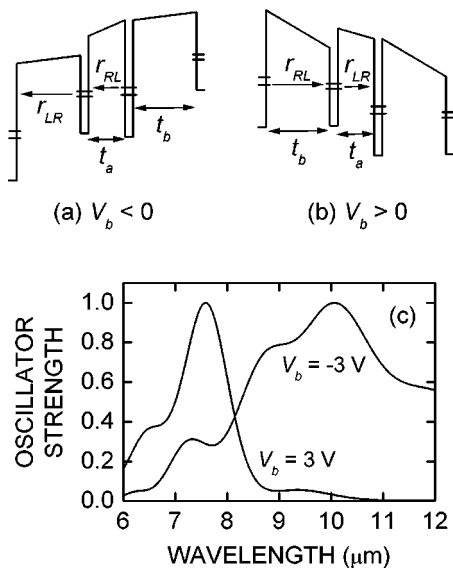


FIG. 1. (a)–(b) Conduction band diagram of a unit cell of the voltage-tunable two-color detector under (a) negative and (b) positive bias V_b . r_{RL} and r_{LR} are the tunneling rates from the RQW to the LQW and from the LQW to the RQW, respectively. The two barriers are $t_a = 200\ \text{\AA}$ and $t_b = 350\ \text{\AA}$ thick. (c) Calculated oscillator strength of intersubband transitions from the RQW at $V_b = 3\text{ V}$ and the LQW at $V_b = -3\text{ V}$.

above them. The normalized values of f are plotted in Fig. 1(c). At bias $V_b = -3\text{ V}$, the $E_1 \rightarrow E_6$ transition within the LQW at $10.1\ \mu\text{m}$ has the largest f (we call this transition $L6$ because E_1 is in the LQW). Other significant transitions are $L7$, $L8$, and $L11$ at 8.9 , 8.3 , and $7.3\ \mu\text{m}$, respectively. At $V_b = 3\text{ V}$, the largest f for the RQW occurs at $7.6\ \mu\text{m}$, which corresponds to the $E_1 \rightarrow E_7$ ($R7$) transition.

We show spectral responsivity R of a 45° -edge coupled detector at different temperatures in Fig. 2. At $T = 10\text{ K}$, λ_p switches from 7.1 to $8.6\ \mu\text{m}$ for $|V_b| \geq 3\text{ V}$ upon reversing the bias polarity. Under positive bias, R is almost independent of T in the 10 – 70 K range. Under negative bias, R has negligible temperature dependence up to 40 K . However, R

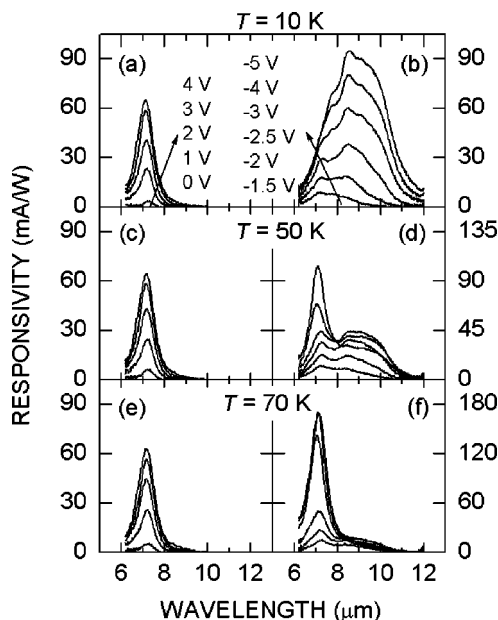


FIG. 2. Spectral responsivity R of 45° -edge coupled detectors at (a), (b) $T = 10\text{ K}$; (c), (d) $T = 50\text{ K}$; and (e), (f) $T = 70\text{ K}$.

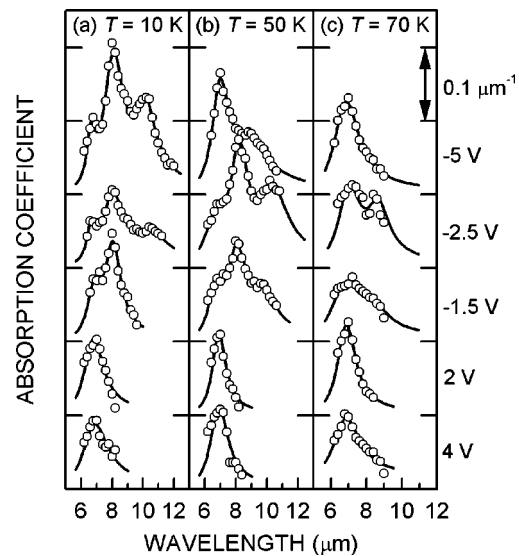


FIG. 3. Spectrum of absorption coefficient α at temperature (a) $T = 10\text{ K}$, (b) $T = 50\text{ K}$, and (c) $T = 70\text{ K}$. Symbols: α obtained from CQWIP data. Lines: least-squares fit of single or multiple Lorentzians to the data shown as circles. Each curve has been shifted by $0.1\ \mu\text{m}^{-1}$ from the one just below it for clarity. The bias voltages V_b are indicated on the right margin. Typical error bars of 10% are not shown for clarity.

changes dramatically once T is raised above 40 K . The shorter wavelength peak at $7.1\ \mu\text{m}$ is not only prominent but also dominant at higher temperatures. This is accompanied by a rapid reduction of the longer wavelength peak.

In order to gain a better understanding of the temperature dependence of detector responsivity, we extracted absorption coefficient α using CQWIPs with different corrugation periods.^{9,10} Details of this approach have been described previously^{6,9,10} and will not be repeated here. The deduced absorption spectra are shown as circles in Fig. 3. For the entire temperature range under positive bias, there is one absorption peak around $7\ \mu\text{m}$ that can be assigned to the $R7$ transition ($\lambda_{R7} = 7.6\ \mu\text{m}$ for nominal detector parameters). Under negative bias at $T = 10\text{ K}$, the main absorption peak is at $8.1\ \mu\text{m}$, which is interpreted as the unresolved $L7$ and $L8$ transitions. There are two smaller peaks at 7 and $10.4\ \mu\text{m}$. The $10.4\ \mu\text{m}$ peak is attributed to the $L6$ transition while the $7\ \mu\text{m}$ peak is still from the previously labeled $R7$ transition in the RQW. Since Stark shifts are small in this structure, the small discrepancies in the locations and magnitudes between the calculated and observed transitions are attributed to differences in the nominal and actual detector structures. These differences, however, do not affect the following data analysis.

The presence of a large $7\ \mu\text{m}$ peak under negative bias, especially at high temperatures, indicates that a significant number of electrons remain in the RQW under negative bias and electron transfer to the LQW is inefficient. We use the absorption spectra shown in Fig. 3 to quantitatively determine the LQW and RQW electron densities, n_L and n_R , respectively. By evaluating the integrated absorption strength (IAS) of the absorption peaks shown in Fig. 3, we can obtain n_L and n_R because the IAS of each transition, denoted by A_T , is proportional to $f_T n_{2D} / m^*$, where f_T , n_{2D} , and m^* are the oscillator strength, QW electron density, and effective mass, respectively. The IAS of the individual transitions is

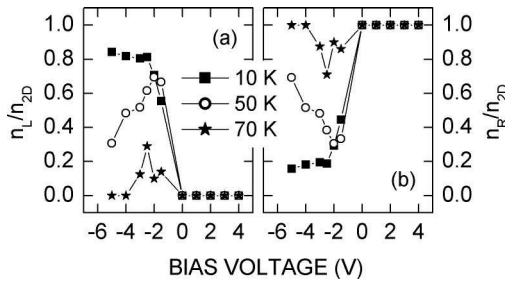


FIG. 4. Two-dimensional (2D) electron density in (a) the LQW n_L/n_{2D} and (b) the RQW n_R/n_{2D} at $T=10, 50,$ and 70 K. The total 2D electron density $n_{2D}=3.1 \times 10^{11} \text{ cm}^{-2}$.

obtained by fitting Lorentzians of the form $\alpha(E) = A_T \Delta E / \{2\pi[(E - E_p)^2 + (\Delta E/2)^2]\}$ to the absorption data. Here E is energy, and the IAS A_T , peak position E_p , and peak width ΔE are fitting parameters. We use one Lorentzian for positive bias and two or three Lorentzians for negative bias to match the number of peaks found in the absorption data. The least-squares fits are shown as solid curves in Fig. 3. Note that we use the peak positions E_p as fitting parameters so that the fitting is independent of the calculated peak positions.

After obtaining the values of A_T for different transitions from the fitting procedure, n_L and n_R are obtained by the following method. Based on the $R7$ transition, n_R and A_{R7} are related by $A_{R7} \propto f_{R7} n_R / m_R^*$, where m_R^* is the effective mass in the RQW. Since both the initial state and the final state of the $R7$ transition are localized in the RQW, the value of f_{R7} is insensitive to both the magnitude and polarity of V_b . On the other hand, under negative bias, the final state wave functions of the LQW transitions are more delocalized throughout the unit cell, and thus, the individual oscillator strengths can change with V_b . Nevertheless, due to the conservation of oscillator strength, the total f of all the prominent LQW transitions will remain relatively constant with V_b . Accordingly, the sum of the IAS of the 8.1 and $10.4 \mu\text{m}$ transitions, denoted by A_L , is proportional to $f_L n_L / m_L^*$, where f_L is the bias-insensitive sum of oscillator strengths of the observed transitions and m_L^* is the effective mass in the LQW. Using the earlier two relations for A_{R7} and A_L with $n_{2D} = n_L + n_R$, where n_{2D} is the total electron density in an unit cell, we obtain $n_L = n_{2D} / (1 + r)$ and $n_R = n_{2D} / (1 + 1/r)$, where $r = m_R^* f_L A_{R7} / m_L^* f_{R7} A_L$. We use the values of A_{R7} and A_L determined from the fitting procedure, the computed ratio f_L / f_{R7} at $|V_b| = 3 \text{ V}$, $m_L^* = 0.0707 m_0$, and $m_R^* = 0.0665 m_0$, where m_0 is the free-electron mass, to determine n_L and n_R . These densities are plotted in Fig. 4 for different temperatures. Figure 4 shows that all electrons are in the RQW at positive bias and that most of them are transferred to the LQW under negative bias at $T=10$ K. However, the transfer becomes less efficient at higher voltages and temperatures.

It is clear from Fig. 1(b) for positive bias that the individual electron transfer rate r_{LR} from the LQW to the RQW is always larger than r_{RL} from the RQW to the LQW of the next unit cell due to the same barrier height. Therefore, thermal equilibrium within the unit cell can be maintained and electrons are transferred to the RQW. On the other hand, due to the graded nature of the thick barrier for thermionic emission (TE) is continuously lowered by negative bias as shown in Fig. 1(a). At sufficiently high bias and temperature where TE is dominant, r_{LR} in Fig. 1(a) becomes larger than r_{RL} due to larger TE transport. In this case, the LQW is actually in thermal equilibrium with the RQW of the next unit cell, resulting in electrons populating the RQW as seen in Fig. 4. In intermediate cases where $r_{LR} \approx r_{RL}$, the two QWs have similar populations as observed at $T=50$ K in Fig. 4. Similar conclusions can also be reached using current continuity where $n_L r_{LR} = n_R r_{RL}$.

In conclusion, we have studied the temperature and bias dependence of electron transfer between coupled QWs in a voltage tunable two-color photodetector. We showed that the electron transfer process is efficient only when interwell tunneling dominates. At higher temperatures when thermionic emission is substantial, electrons tend to accumulate in the shorter wavelength QW, which has a higher thermal activation energy, under most bias voltages due to the smaller electron transfer rate out of that QW.

The work at Princeton University is supported by grants from the Army Research Office and the National Science Foundation. Sandia is a multiprogram laboratory operated by Sandia Corporation, a Lockheed Martin Company, for the United States Department of Energy under Contract No. DE-AC04-94AL85000.

¹K. K. Choi, *The Physics of Quantum Well Infrared Photodetectors* (World Scientific, River Edge, NJ, 1997).

²*QWIP 2000*, edited by S. D. Gunapala, H. C. Liu, and H. Schneider (Elsevier, New York, 2001).

³S. R. Parihar, S. A. Lyon, M. Santos, and M. Shayegan, *Appl. Phys. Lett.* **55**, 2417 (1989).

⁴K. K. Choi, B. F. Levine, C. G. Bethea, J. Walker, and R. J. Malik, *Appl. Phys. Lett.* **52**, 1979 (1988).

⁵V. Berger, N. Vodjdani, P. Bois, B. Vinter, and S. Delaire, *Appl. Phys. Lett.* **61**, 1898 (1992).

⁶A. Majumdar, K. K. Choi, L. P. Rokhinson, and D. C. Tsui, *Appl. Phys. Lett.* **80**, 538 (2002).

⁷A. Majumdar, K. K. Choi, L. P. Rokhinson, J. L. Reno, and D. C. Tsui, *J. Appl. Phys.* **91**, 4623 (2002).

⁸A. Majumdar, K. K. Choi, J. L. Reno, L. P. Rokhinson, and D. C. Tsui, *Appl. Phys. Lett.* **80**, 707 (2002).

⁹C. J. Chen, K. K. Choi, M. Z. Tidrow, and D. C. Tsui, *Appl. Phys. Lett.* **68**, 1446 (1996).

¹⁰K. K. Choi, C. J. Chen, and D. C. Tsui, *J. Appl. Phys.* **88**, 1612 (2000).